

Infrared Observations of the Eclipsed Moon From Space



Dr. Stephan D. Price
Space Vehicles Directorate
Air Force Research Laboratory

The disk resolved 4.3 μm thermal emission profile of the Moon was measured during the eclipse of 26 September 1996 by the SPIRIT III sensor on the Midcourse Space Experiment (MSX). This is the first experiment to measure the thermal properties of the Moon after an almost 25 year hiatus in a series of experiments that was sponsored or conducted by the Air Force Research Laboratory and its component predecessor agencies the Air Force Cambridge Research Laboratories (AFCRL) and the Air Force Office of Scientific Research. Shorthill¹ reviewed the thermal measurements in the 1960s conducted under the aegis of AFRCL. Shorthill and colleagues, then of the Boeing Scientific Research Laboratories and under contract to AFCRL, observed the thermal time profile at $\sim 11 \mu\text{m}$ during eclipses of 13 March 1960² and 19 December 1964³; Salisbury's group at AFCRL obtained mid-infrared images of the 13 April 1968 eclipse⁴. Shorthill's group also imaged the full Moon in the mid-infrared and obtained thermal profiles during several lunations (night and day).

¹Shorthill, R., 1972, The Infrared Moon: A Review. In *Thermal Characteristics of the Moon*, J. Lucas (ed.) MIT Press, Cambridge MA, 3 – 79.

²Shorthill, R.W., H.C. Borough and J.M. Conley, 1960, Enhanced Lunar Thermal Radiation During a Lunar Eclipse. Pub. Astron. Soc. Pac. **72**, 481 – 485.

³Saari, J.M., R.W. Shorthill and T.K. Deaton, 1996, Infrared and Visible Images of the Eclipsed Moon of December 19, 1964. *Icarus*, **5**, 635 – 659.

⁴Hunt, G.R., J.W. Salisbury and R.K. Vincent, 1968 “Lunar Eclipse: Infrared Images and an Anomaly of Possible Internal Origin,” *Science*, **162**, 223 – 225.



Introduction



- Space craft and infrared sensor
 - MSX – multi-objective BMDO experiment
 - SPIRIT II
 - Line scanned radiometer
- The experiment
 - 3 observations of the 26 Sep 1996 lunar eclipse
 - 10 partial images of the Moon during each observation
- Results
 - Numerous hot spots – seen previously in mid-IR
 - Time and disk resolved cooling profiles

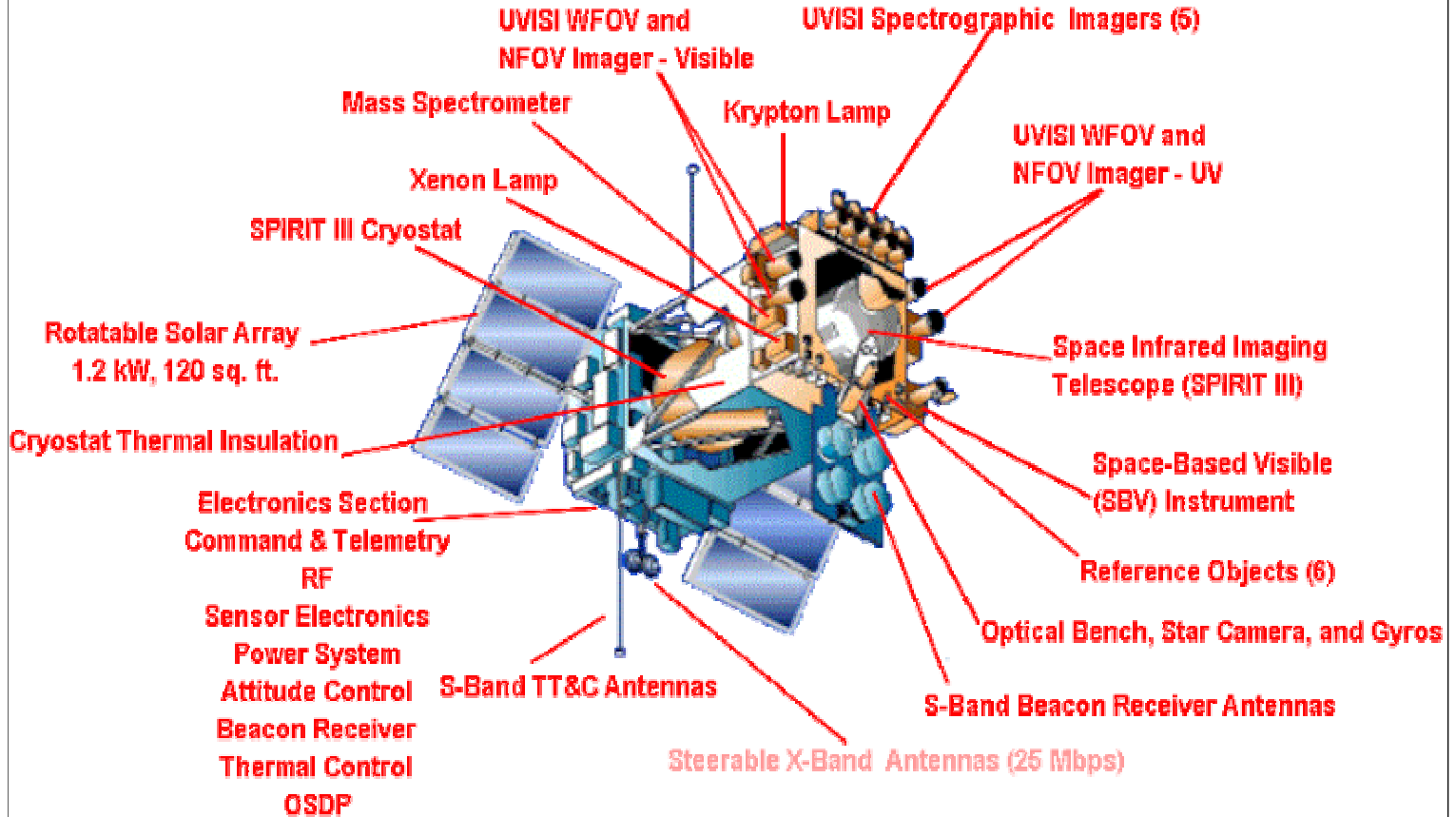
2

The Midcourse Space Experiment (MSX) mapped the thermal $4.3 \mu\text{m}$ emission from the Moon during the 27 September 1996 eclipse at a resolution of about $30''$. MSX obtained $4.3 \mu\text{m}$ brightness temperatures every 1 to 3 minutes during three observations of the eclipse and was thus able to define disk resolved (45km) cooling curves over the entire surface of the Moon. The temperature contrasts observed for various regions during eclipse agree well with those previously published, although there is a tendency for the MSX $4.3 \mu\text{m}$ values to be $\sim 20\text{K}$ warmer. A large number of “hot spots” were observed, which correlate well with those noted by previous observers. Most of the warm discrete spots correspond to craters. The maria, and portions thereof, tend to be warmer than the highlands. This database on the details of the non-uniform cooling during the eclipse provide information on the thermo-physical properties of the various features on the surface of the Moon.

The only previous published infrared maps of the entire Moon during eclipse at relatively high spatial resolution are those at $11 \mu\text{m}$ obtained by Shorthill² and by Saari et al.³ of the 19 December 1964 eclipse. They raster scanned a $10''$ beam across the Moon, taking ~ 16 minutes to complete a map. They noted hundreds of areas perceptively warmer than the surroundings, which they labeled as anomalies. They also found that the maria, or portions of maria, were warmer than the disk averaged temperature. Hunt et al.⁴ mapped about 70% of the Moon during the 13 April 1968 eclipse at $10 \mu\text{m}$, looking for changes in the relative intensities of the anomalies between the epochs of the two eclipses, which they did not find. The MSX measurements are of lower spatial resolution, but the data are not aliased and each lunar observation is a snap-shot of only 10 seconds in duration.



The MSX Satellite



3

MSX was a Ballistic Missile Defense Organization satellite with multiple disciplinary experimental objectives. Mill et al.⁵ give an overview of the spacecraft, instruments and mission objectives.

The MSX spacecraft measures about 1.5x1.5x5.1 meters with a mass of 2.7 tons and supports four sets of electro-optical sensors. It is somewhat modular in construction giving it the rather ungainly appearance. The primary mission instrument was an infrared sensor, designated SPIRIT III for historical reasons, mounted at the center of the spacecraft. Arrayed around SPIRIT III are the four ultraviolet-visible imaging telescopes (UVISI) and the five ultraviolet to far red hyperspectral imaging instruments. Off to the side is the 20 cm Space-Based Visible (SBV) surveillance telescope. All the electro-optical sensors are referenced to the optical reference plane at the front of the spacecraft and boresighted with the SPIRIT III telescope.

MSX was launched on 24 April 1996 into a ~900 km polar orbit. The first phase or infrared portion of the mission terminated on 20 February 1997, when the radiometer focal plane temperatures reached 13K. For the year following cryogen loss, Phase 2 emphasized astronomy and atmospheric measurements with the ultraviolet-far red sensors.

⁵Mill, J.D., R.R. O'Neil, S. Price, G.J. Romick, O.M. Uy, E.M. Gaposchkin, G.C. Light, W.W. Moore Jr., T.L. Murdock and A.T. Stair Jr., "Midcourse Space Experiment: Introduction to the Spacecraft, Instruments and Scientific Objectives," *J. Spacecraft and Rockets*, **31**, 900-907, 1994.

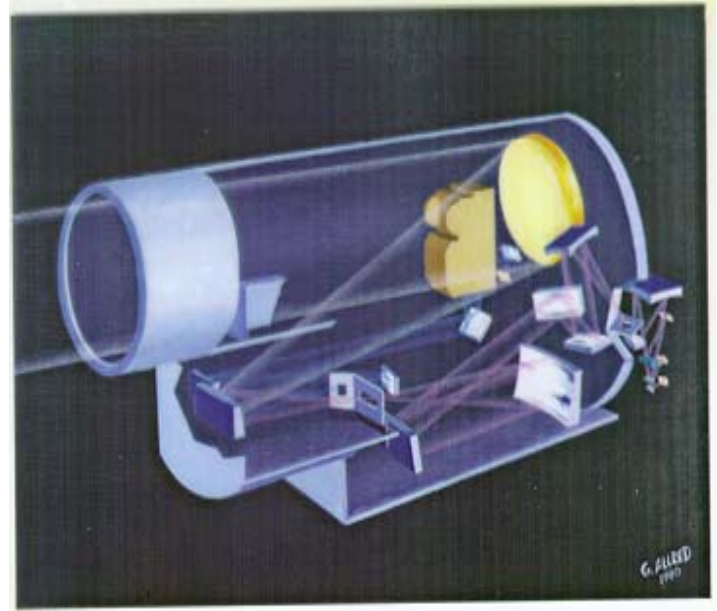


The MSX IR Sensor



- Telescope and FPA's

- aspheric off-axis optics
- 33 cm unobscured aperture
- 5 Si:As detector arrays
 - 18.3 arc sec square pixels
 - 9.15" cross-scan sampling
 - 1° cross-scan fov
- 3 - 26 μm interferometer
 - 6 detectors
 - 2 to 20 cm^{-1} resolution



- 944 liter solid H_2 dewar

- ~ 10 months on-orbit lifetime
 - 4/24/96 launch - 2/26/97 EOL

- Data Acquisition

- 0.05°/sec scan rate
- 5Mps data rate

4

The MSX Infrared sensor was built by the Space Dynamics Laboratory of the Utah State University. This off-axis telescope had a 33 cm clear aperture and a 896 cm^2 collecting area. The optics exceeded the design requirement to be diffraction limited at 12 μm to which the detectors were sized. The focal plane radiometer sub-assembly contained five line-scanned infrared focal plane array. The entire system was cooled by a 944 liter solid H_2 cryostat. The Si:As focal plane arrays had eight columns of detectors, each consisting of 192 rows of 18.3" square pixels. Half the columns were offset by half a pixel, providing critical sampling in the cross scan direction. To reduce the telemetry rate, only half the columns were active but at least one column was active on either side of the stagger.

The 4.3 μm spectral band was divided in cross-scan by two different near-infrared filters centered on the 4.3 μm atmospheric CO_2 band. These near-infrared bands had isophotal wavelengths and bandwidths of $\lambda = 4.29 \mu\text{m}$, $\Delta\lambda = 0.104 \mu\text{m}$ and $\lambda = 4.25 \mu\text{m}$, $\Delta\lambda = 0.179 \mu\text{m}$. The effective beam size for each bands was measured to be 140 μsr and the full width at half maximum response was about 23". Thus, the resolution was about 30" and the data were adequately sampled by the half detector cross-scan offset of the two columns that were active for this focal plane array and by the seven in-scan data samples per dwell time on a detector. The filter mask in the center of the array limited the field of view of the individual sub-arrays to 0.4°.



The Experiment



- Three data collection events
 - 50 Minutes apart
 - Beginning and end of totality, Moon half sunlit
 - 10 scans across the Moon
 - Lunar maps ~1 and ~3 minutes apart
- 4.3 μm narrow band data
 - Two bands
 - 4.22 – 4.36 μm
 - 4.24 – 4.45 μm
 - 18.3'' square detectors, ~30'' resolution

5

The sensor was extensively calibrated in a specially built vacuum chamber on the ground and on orbit. A sapphire blocking filter eliminated the out of band spectral response for wavelengths greater than 6.5 μm , resulting in negligible long wavelength contamination (less than 1% for a 200K blackbody). The small out of band response was confirmed by the fact that the in-orbit calibration produced only minor adjustments to the 4.3 μm responsivities derived from the ground calibration. The ground calibration used a flat plate with temperatures similar to the eclipsed Moon while the on orbit calibration sources⁶ were stellar standard with $T_{\text{eff}} > 4000\text{K}$. The effective solid angles in the two near infrared bands were measured by repeated raster scans across stellar point source calibration standards and are estimated to have an uncertainty of < 8%.

The thermal input from the Moon raises the focal plane temperature by a small amount, which increases the dark offset in a quasi-asymptotic fashion. A dark offset was measured every two minutes, at the end of each scan leg, and linear fits between the measured values for successive offsets for each detector are used to interpolate to the time of observation. The maximum offset bias is estimated from the deviation of the measured offsets from a monotonic trend to be comparable to the rms noise in the measurement. This is equivalent to about a 2K bias at 180K and much smaller at higher brightness temperatures.

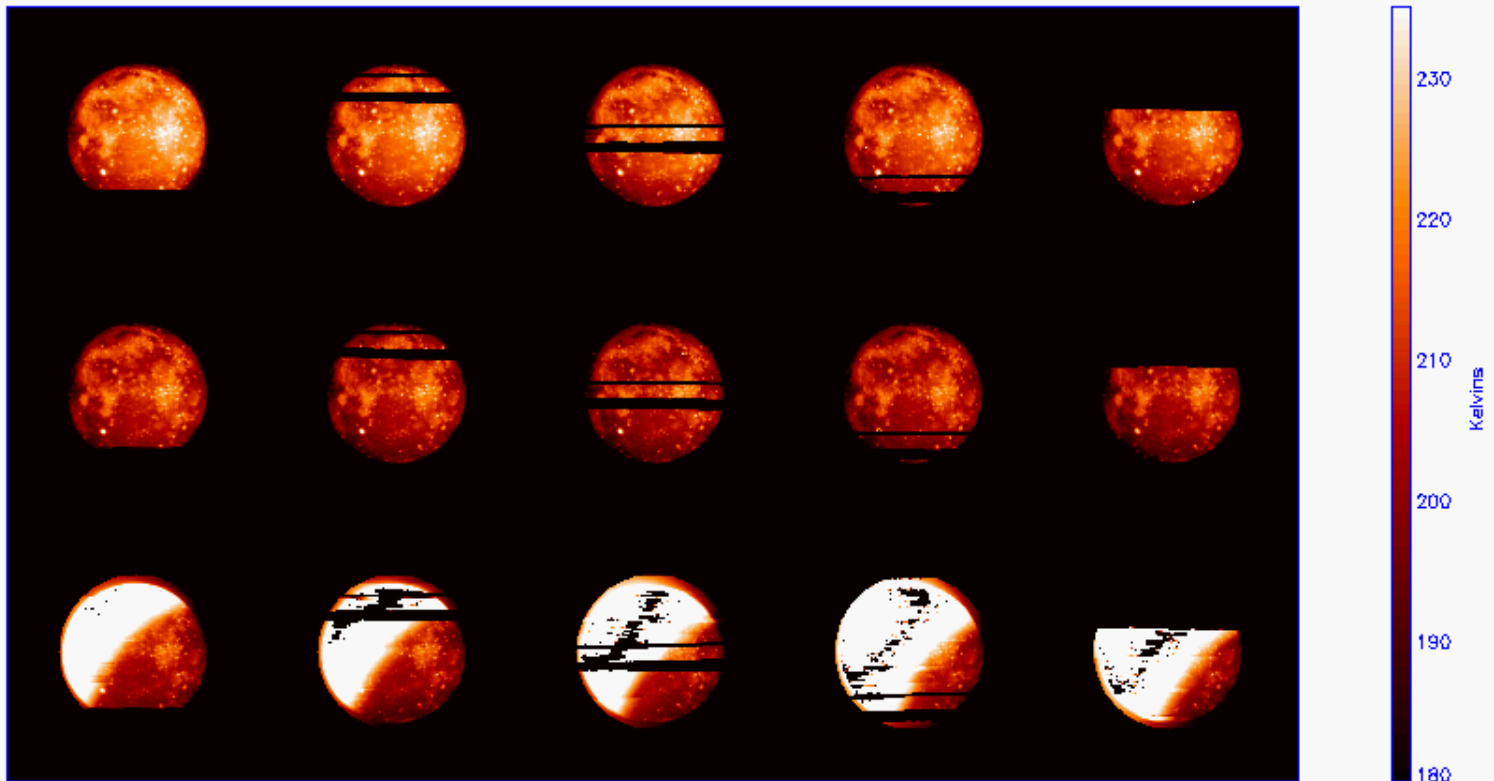
⁶ Burdick, S.V., and D.C. Morris, "SPIRIT III Calibration Stars: In-Band Irradiance and Uncertainty." Opt. Eng. 36, 2931 – 2931.



4.3 μm Maps of the Eclipse



Band B Brightness Temperatures



6

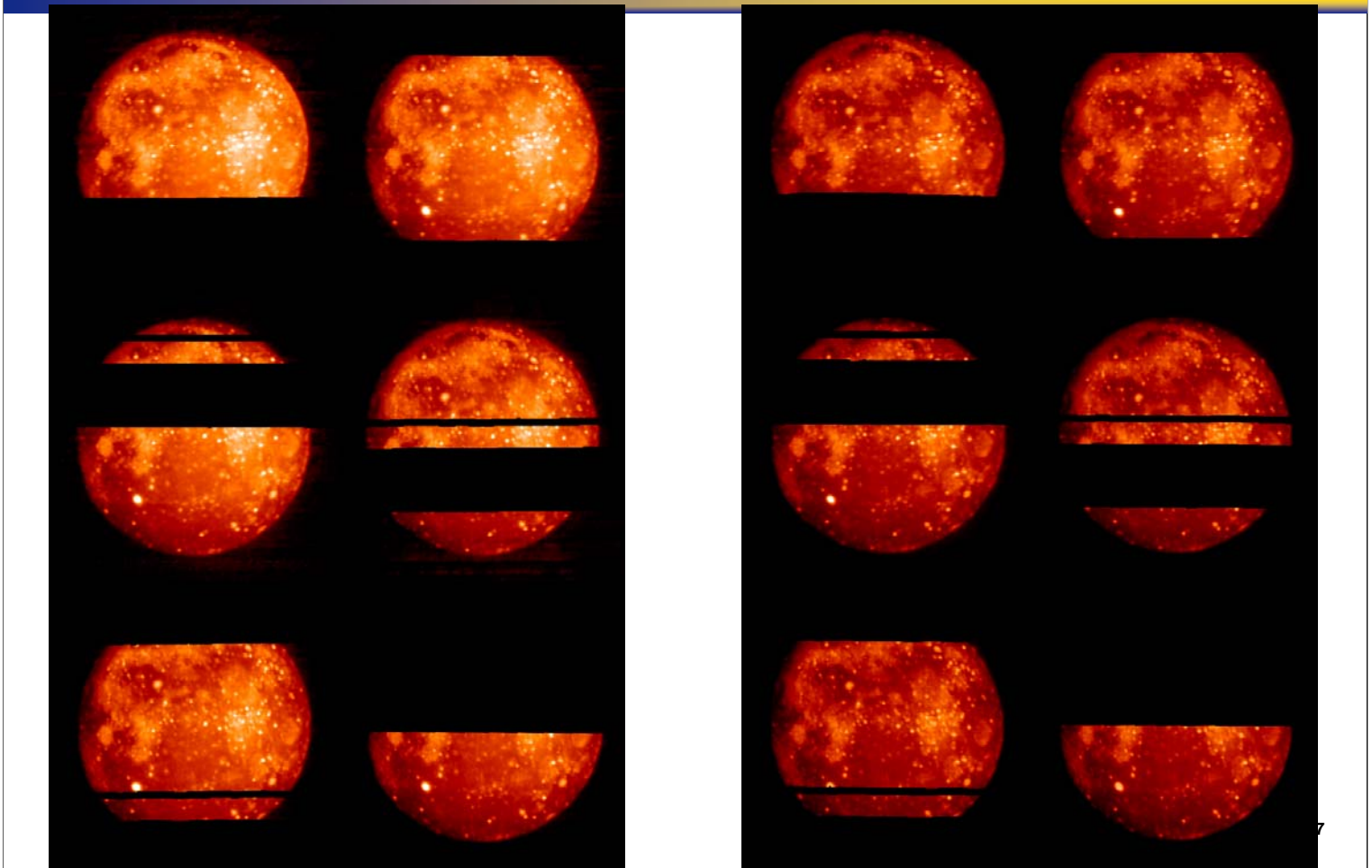
The eclipse was observed on three data collection events (DCEs) spaced about 50 minutes apart. Each 20 minute DCE obtained ten 6° long raster scans at a scan rate of $0.05^\circ/\text{sec}$. The satellite was stepped 0.05° in cross scan at the end of each raster leg while the dark offset was being measured with the internal shutter closed.

The Moon was scanned near the beginning of the odd numbered scans and the end of the even numbered scans. Thus, successive scans across the Moon were alternately spaced by about 3 and 1 minute apart. Only about two-thirds of the Moon was within the field of view of the two near infrared arrays on each scan. Therefore, the first scan was oriented such that the edge of the Moon is just within the outer edge of the array and successive raster legs were offset by 0.05° in the cross-scan direction. Thus, the Moon was walked across each sub-array during the DCE. The observations were converted into brightness temperatures, mapped onto a flat plane projection with $6''$ spacing and selenographic coordinates assigned to each grid element. The positional accuracy of the result was roughly 0.5° and 1.0° in selenographic latitude and longitude, respectively, which is consistent with the resolution of the observations and the pointing accuracy of the system. The formal 5% uncertainty in the radiance calibration translates to a $\sim 1\text{K}$ uncertainty in the brightness temperature.

Above is a montage of images from all three DCEs, in which the data from two successive legs were combined. The data do not overlap owing to the 0.2° gap caused by the focal plane mask separating the two $4.3 \mu\text{m}$ spectral bands. The narrower black line is due to a group of dead detectors in one of the bands.



Beginning and End of Totality



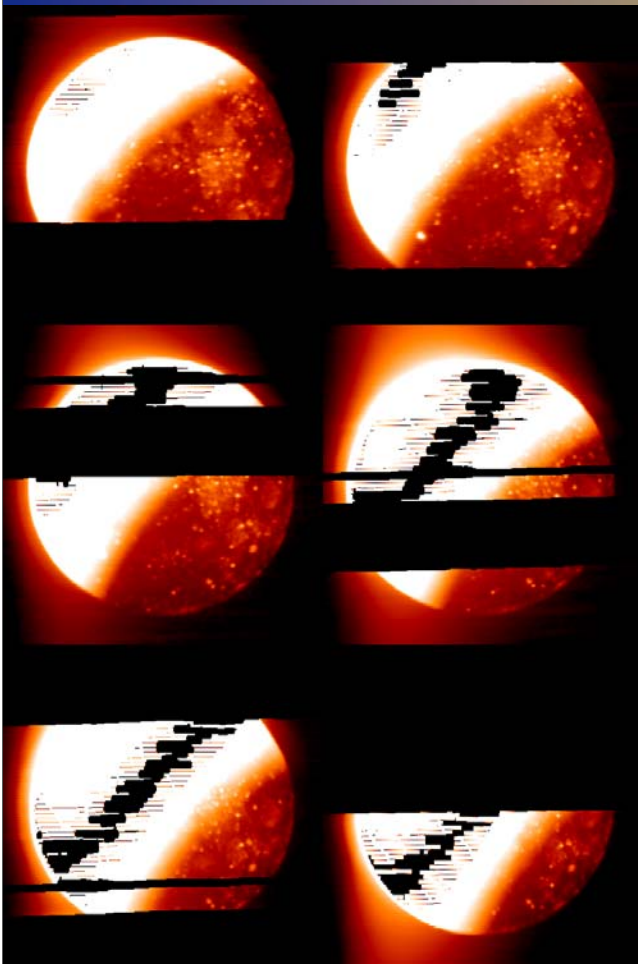
At left are larger images of the data taken during the first DCE just as the Moon enters totality, while the right panel shows the images from the second DCE, which observed the Moon just as totality ends. Images created from the first and last scan appear in the upper left and lower right of each panel. Here, measurements taken at the end of the even scans were combined with those at the beginning of the following odd scans to create the middle four images. This pairing combines data that are separated by only about a minute in time.

As can be seen, the Moon perceptively cools as the eclipse progresses. Also evident are the numerous hot spots, labeled anomalous by previous investigators. The brightest of these anomalies are associated with craters, Tycho and Copernicus being the brightest. However, the maria on the Moon are clearly defined and are at an elevated temperature, which is expected given the grain sizes¹ and the relatively low albedos. The highlands are relatively cool because their albedo is high. The coolest temperatures are to the lower right of Tycho, limb-ward and above Mare Humorum and the Jura mountains. The craters, especially the rayed craters, also have a relatively high albedo but are warm owing to the thermo-physical characteristics of their rough floors and the fact that the walls of the craters “trap” heat.

Shorthill¹ says that there are over 1000 anomalies, or hot spots that are distinct, detectable features of the mid-infrared infrared maps obtained either during eclipse or the lunar night. These mid-infrared features correlate well with those at 4.3 μm (compare the figures in view graphs 8 and 9.)



Last Observation



Observation Times		
	Begin	End
Totality	2^h 19.3^m	3^h 29.4^m
DC35_02	2^h 12.6^m	2^h 41.7^m
DC35_03	3^h 05.1^m	3^h 34.2^m
DC35_04	3^h 57.1^m	4^h 24.9^m

8

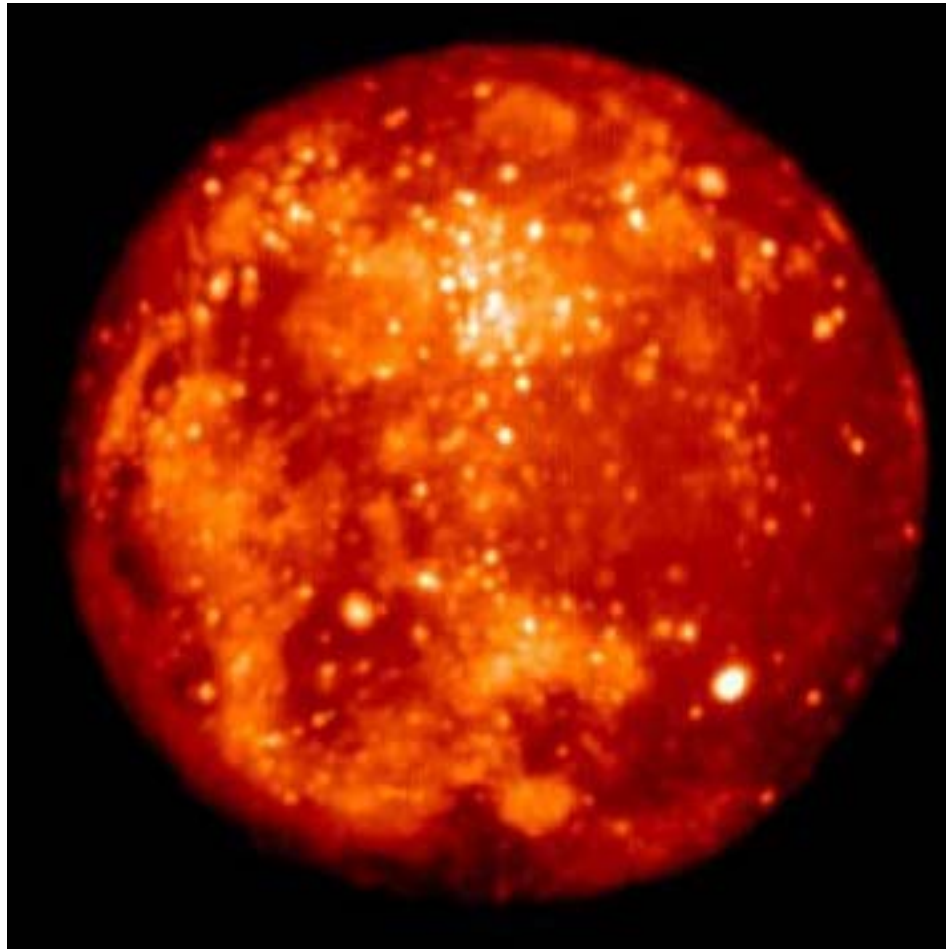
Images created from the third DCE when about half the Moon was sunlit are shown above. The temperatures for the portion of the Moon that are still in eclipse continue to decline, while the temperatures on the sunlit side of the Moon rise rapidly. The 4.3 μm spectral bands go into soft saturation, which is designated by the white region. The black band are regions with the warmest temperatures and are hard saturated.

Interference filters such as the ones used for the 4.3 μm arrays scatter radiation from a bright sources⁷ and such scattering for the 4.3 μm filters was mapped in detail during the ground calibration. The scattering is evident by the band of lighter color between the eclipsed and sunlit portions of the Moon as well as the response outside the edge of the lunar disk. Scattering would most strongly effect the brightness temperature contrast between the bright craters and their immediate surrounding. The ground calibration indicates that the scattering decreasing rapidly in the cross-scan direction with a Lorentzian profile with a characteristic width of 5". A correction to the scattering contribution has been applied to the final data products and the brightness temperature maps displayed in view graph 12. The correction changed the brightness temperatures of the brighter regions by $< 2^\circ \text{K}$ while the coolest regions are more strongly effected with as much as a 10K decrease for measurements just above the noise floor.

⁷Stierwalt, D.L., and W.J. Eisenman, 1978, Problems in using cold spectral filters with LWIR detectors, Proc. SPIE, 132, 134 – 140.



Averaged 4.3 Map



9

The 4.3 μm image of the average of all the measurements taken during the last 20 minutes of totality. The image has been rotated counterclockwise by 90° to bring it into closer alignment with the visual image of the full Moon in view graph 9, which is included for comparison.

The brightness temperature on the Moon drops steeply during the partial phase of eclipse from about 380K to $\sim 200\text{K}$ for the sub-solar point. Thereafter, it declines less steeply to $\sim 175\text{K}$ by the end of totality⁸. Fairly large local contrast exist. For example, Shorthill, Borough and Conley⁹ determined that the lunar disk temperature dropped to below 200K during the eclipse of 13 March 1960 and that Tycho was about 50K warmer than its surroundings. Saari, Shorthill and Deaton¹⁰ produces an isothermal contour map of the Tycho region that also had about a 50K contrast with the crater at a temperature of roughly 210K and the surrounding at about 160K near the end of totality. These temperatures are in qualitative agreement with the 8.3 μm image where anything that is not black (saturated) should be cooler than 195K; but are about 20K lower than the values observed at 4.3 μm

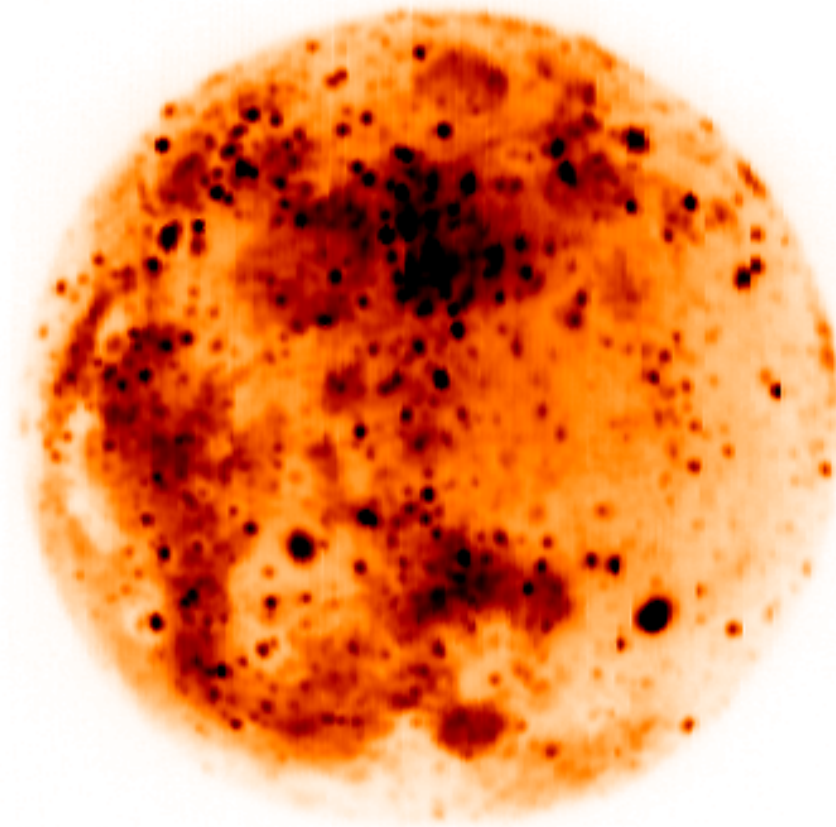
⁸Petit, E., 1940, "Radiation Measurements on the Eclipsed Moon," *Astrophys. J.*, **91**, 408 – 420.

⁹Shorthill, R.W., H.C. Borough and J.M. Conley, 1960, "Enhanced Lunar Thermal Radiation During a Lunar Eclipse," *Pub. Astron. Soc. Pac.*, **72**, 481 – 485.

¹⁰Saari, J.M., R.W. Shorthill and T.K. Deaton, 1966, "Infrared and Visible Images of the Eclipsed Moon of December 19, 1964," *Icarus*, **5**, 635 – 659.



Averaged 8.3 μm Map



The MSX 8.3 μm (isophotal wavelength) band had an isophotal bandwidth of $\Delta\lambda = 3.3 \mu\text{m}$, and a system response above 50% from 6.8 to 10.8 μm . Measurements of the eclipsed Moon in this band were saturated during all three DCEs. However, a peculiarity of the read-out electronics for this band was that the response had a soft saturation regime. The detector response would reach a maximum then fold back, or decrease, with increasing flux with a gain decrease of about a factor of four until it went into hard saturation at zero counts. Data from the ground calibration indicates that the soft saturation response for this band spanned a ~150K to 195K dynamic range in brightness temperature. We attempted to correlate this fold back response with brightness temperatures derived from the 4.3 μm observations, but could not do so to our satisfaction as the scatter was too large. However, the 8.3 μm images can be used for qualitative correlation. One such inference in comparing this and the 4.3 μm map is that the mid-infrared brightness temperatures across the Moon is, on the average, roughly 20K cooler than those derived from the near infrared measurements

About 20% of the Moon is hard saturated in this band. The saturated, black areas are at temperatures above 195K and are mainly warm craters. The concentration of craters in the areas of Mare Tranquillitatus and Serenitatus and the low albedos for these regions result in this area having the most saturation. The coolest temperatures are for the south eastern limb of the Moon and the area northwest of Mare Humorum.



The Visible Full Moon



11

The discrepancy between mid- and near infrared observations could be brought into accord if the $4.3\ \mu\text{m}$ emissivity of the Moon was ~65% higher than that in the mid-infrared. This is, of course, at odds with the usual assumption that the Moon is grey with an emissivity of 0.9. However, Murcray et al.¹¹ measured a wavelength dependent emissivity between $7 - 13.5\ \mu\text{m}$ for six regions of the nearly full during a balloon flight on 13 April 1868. Vogler et al.¹² corrected the Murcray et al. results for the residual atmospheric absorption above the balloon and found that the normalized emissivity varied from 90% at $13.5\ \mu\text{m}$ to 105% at $7\ \mu\text{m}$. Murcray¹³ also observed a 30° latitudinal strip of the full Moon in September and October 1964 in three spectral bands between 8.4 and $11\ \mu\text{m}$ and determined that the energy distribution was wider than a single temperature blackbody. Vogler et al.¹² inferred from these results that the partial disk integrated brightness temperature of the full Moon has a mid-infrared slope of $-3\text{K}/\mu\text{m}$. While it is perilous to extrapolate these observations by a factor of two in wavelength and then to apply the results to the eclipsed Moon, the observed trend is in the correct sense to account for the $4.3\ \mu\text{m}$ brightness temperature measurements.

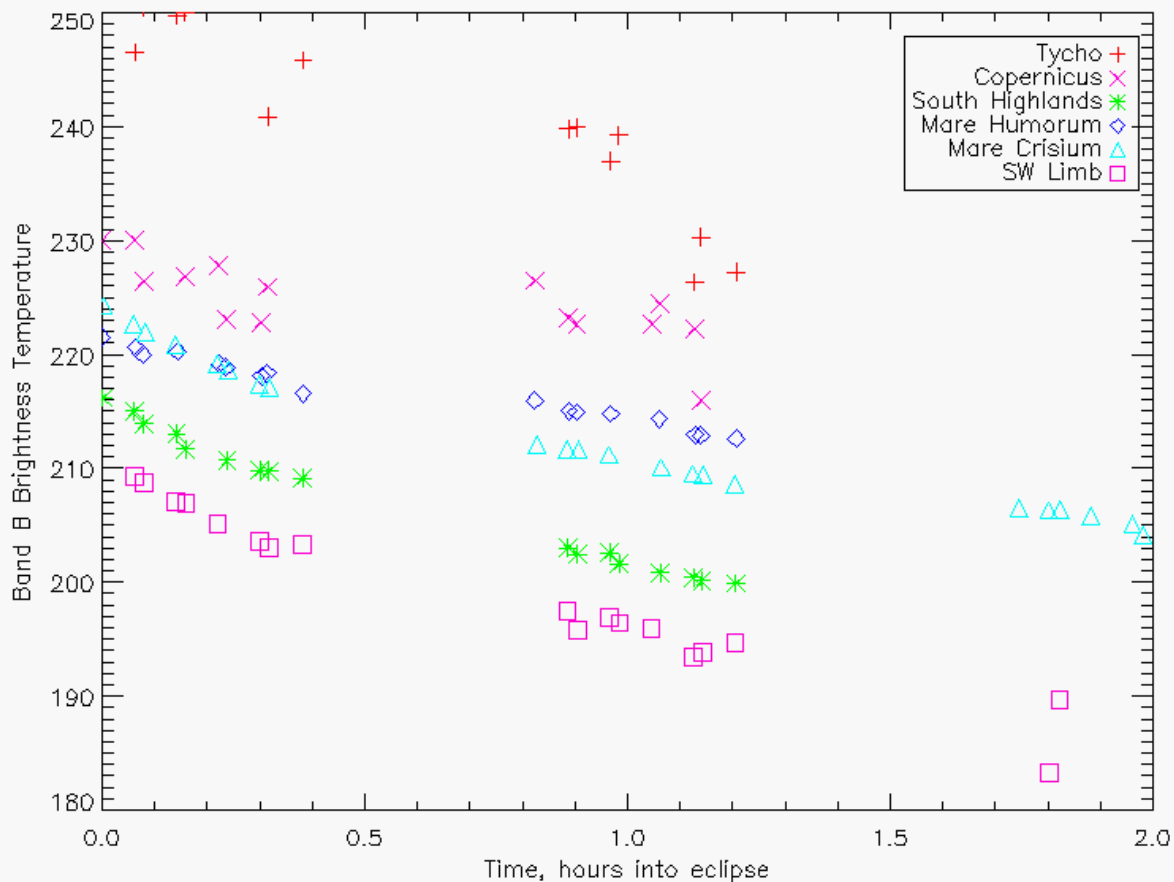
¹¹ Murcray, F.H., D.G. Murcray and W.J. Williams 1970. Infrared emissivities of lunar surface features. Balloon observations, *J. Geophys. Res.* **75**, 2662 – 2669.

¹² Vogler, K.J., P.E. Johnson and R.W. Shorthill 1991, Modeling the Non-Grey-Body Thermal Emission From the Full Moon. *Icarus* **92**, 80 – 93.

¹³ Murcray, F.H., 1965, The spectral dependence of lunar emissivity, *J. Geophys. Res.* **70**, 4959 – 4962.



Thermal Profile of Features



12

The thermal profile for various regions of the Moon during the eclipse is shown above. Each data point for a given feature is the brightness temperature measured on an individual scan; the spacing graphically shows the time resolution of the data. The first data point for Mare Crisium is at a time just after it has entered the Earth's shadow. All the other features are in the lunar western hemisphere and have been in shadow for 20 to 40 minutes. The data labeled SW Limb refers to a point about 10% of the radius from the limb at a position angle of about 80° in view graphs 9 and 10. This is not the coolest area but was chosen because it remains in shadow during the last DCE and data are available from all three DCEs.

The $4.3 \mu\text{m}$ brightness temperatures are as much as 40K warmer than those derived from mid-IR maps. As an extreme example, Saari and Shorthill¹⁴ measured a 170K mid-IR brightness temperature for Mare Humorum, which is $\sim 40\text{K}$ cooler than the $4.3 \mu\text{m}$ value above. The difference appears to be real as likely additional flux contributions from the out of band spectral response and the uncertainties in the effective solid angle, the dark offset and scattering correction are of the order of the 5% absolute calibration uncertainty. A 5% flux uncertainty corresponds to 1K in brightness temperature. The $4.3 \mu\text{m}$ flux has to change by a factor of two in order to decrease brightness temperature by 10K.

¹⁴Saari, J.M., R.W. Shorthill, 1965, Review of Lunar Infrared Observations, in Physics of the Moon: Science and Tech Ser., 13, Amer. Astronaut. Soc. (Pub, Tarzana CA).



Results



- Numerous hot spots
 - Correlates well with previous mid-IR meas.
 - Cools more slowly than surroundings
 - Correlates and anti-correlates with visual albedo
- 4.3 μm brightness T $\sim 20\text{K}$ higher than Mid-IR
 - Effective emissivity $\sim 65\%$ higher than mid-IR
 - Caused by surface roughness and cratering?
 - Warm temperatures contribute more than cooler temperatures to the beam integrated flux at the short wavelengths on the Wien side of the blackbody curve than at longer wavelengths where the response is a less steep function of temperature

13

Conclusions: The Midcourse Space Experiment observed the 27 September 1996 lunar eclipse at 4.3 μm . The observations resolve the lunar disk with a $\sim 45\text{km}$ footprint. Numerous hot spots were detected as were extended features with brightness temperatures significantly warmer than their surroundings. The hot spots and features correlate well with previous mid-infrared measurements. However, the 4.3 μm brightness temperatures are, on the average, 20K warmer than those derived from mid-infrared observations. Vogler et al. account for the observed decrease in brightness temperature with increasing mid-infrared wavelength for the full Moon as due to surface roughness, which they represent by a distribution of parabolic shaped craters across the surface. In the simple example they give, a low spatial resolution measurement of the lunar surface cannot resolve the individual rough features, which tend to be warmer than their surroundings. The measurement beam integrates over features with a range of temperatures. Since the blackbody energy distribution is a steep non-linear function of temperature for the shorter wavelengths, the result is a higher brightness temperature as the warmer areas will contribute much more to the average. The contribution is roughly linear of temperatures at the longer wavelengths, resulting in a lower brightness temperature.